ION SOURCE AND INJECTOR DEVELOPMENT

C. D. Curtis
Fermi National Accelerator Laboratory*
Batavia, Ill 60510

Introduction

This is a survey of low energy accelerators which inject into proton linacs. Laboratories convered include Argonne, Brookhaven, CERN, Chalk River, Fermi, ITEP, KEK, Rutherford, and Saclay. A few laboratories are missing whose data had not reached the author.

At the 1972 Linac Conference, Th. Sluyters presented a review of ion sources for most of these laboratories and compared sources in terms of descriptive features and beam performance.[1] Few changes have occurred since that time. Consequently, this paper emphasizes complete injector systems, comparing significant hardware features and beam performance data, including recent additions.

There is increased activity now in the acceleration of polarized protons, H^+ and H^-, and of unpolarized H^-. New source development and programs for these ion beams is outlined at the end of the report. Heavy-ion sources are not included.

Comparison of Systems

Because of space limitations, no descriptions are given for component systems such as the high-voltage power supply, source electronics, controls, and vacuum. Parameters are given for ion sources in Table I, accelerating columns in Table II and transport lines in Table III. Beam performance data are reserved for Table IV, where a consistent set of numbers is given for a particular operating beam current throughout the system including the linac. Beam emittance is, of course, a measure of beam quality. We use it here, although with a word of caution. For comparison of beams at different laboratories, it can sometimes be misleading for two reasons. Methods of measurement are sometimes different and do not measure identical quantities, and the measurement frequently is not accurate to more than one significant figure. Although design goals are seldom the same in terms of beam current, duty factor, tolerable beam loss, etc., and do vary greatly from one laboratory to another, beam brightness and intensity are of general interest. With these disclaimers we now examine beam performance in detail in relation to current and emittance values. The reader may wish to examine certain construction details in Tables I-III in correlation with the performance data.

Figure 1 plots beam emittance for the 90% contour both at the input and output of Alvarez linacs as a function of the injector current measured at the linac input for eight laboratories and eleven beam conditions. The newer injectors at CERN, Chalk River and Rutherford are not represented in this graph because of presently incomplete performance data. The two data points for Los Alamos are for collimated beams, both deriving from the same initial column beam of 22mA. The severely collimated beam of 2.1mA is standard operation to meet their present requirements. All data presented in graphical form come from standard proton beams only.

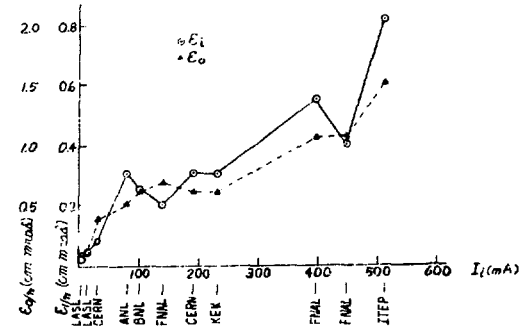

Fig. 1. Beam emittance at entrance and exit of linac versus input current.

The emittance both into and out of the linac is a generally increasing function of the input beam current in Fig. 1. The same data are shown in another way in Fig. 2. Plotted are ratios of output to input emittance and output to input brightness versus input brightness at the various laboratories. No error bars are shown but could be large enough to minimize the importance of at least the smaller fluctuations from one point to another. There seems to remain, however, a slow general increase in emittance growth and in brightness dilution with increasing brightness of the input beam. That this trend is true for each linac does not necessarily follow, but is probably true. At Fermilab these and other data suggest the same trend. A practical consequence of this trend is that an improvement in emittance or brightness of the injector beam gives an improvement, however smaller, in the linac beam.

*Operated by Universities Research Association Inc. under contract with the Energy Research and Development Administration.

TABLE I

ION SOURCE

Laboratory	Argonne	Brookhaven	CERN	Chalk River	Fermilab
Type of Source	Duoplasmatron	Duoplasmatron	Duoplasmatron	Duoplasmatron	Duoplasmatron
Hydrogen Pressure (Torr)	0.3	0.2 - 0.5	0.5	~0.3	~0.15
Arc Current (Amperes)	40-50	10-25	70-90	6-15	60-80
Maximum Magnetic Field (kG)	3	2-5	8	1	3
Source Aperture (mm)	0.6	1.3	0.6	0.5-1.0	1.3
Plasma Expansion Cup					
Exit Diam. x Length(mm x mm)	13 x 24	22.2 x 24.6	20 x 61	19 x 14	{27 x 75 / 41 x 75 / 31 x 75} *
Wall Bias (Volts)	0	0	-30	Insulating Liner	-100**
Cathode Type	RCA J1855 Indir. Heated Matrix	Oxide on Ni Gauze	Oxide on Ni	Oxide on Ni Gauze	Oxide on Ni Gauze
Duty Factor of Arc	0.5×10^{-4}	4×10^{-3}	1.2×10^{-4}	100%	$2\text{-}3 \times 10^{-4}$
Lifetime of Source (hours)	5000-10000	~6000	>1 year	>250 hrs @ 100mA	3000-8000
Common Cause of Failure	Cathode	Cathode	-	Cathode	Cathode
Extraction					
Directly into Column Field	Direct	Direct	Direct	Direct	Direct
Into Focussing Lens Section Extraction Voltage (kV)		30(up to 45)		10-35	43-65
Other Distinctive Source Features		Molybdenum disk on arc side of anode aperture is critical factor in transporting plasma through cup.			*Three cup sizes to match three column apertures. **Cup bias is pulsed to shape the beam pulse.

Laboratory	ITEP	KEK	Los Alamos	Rutherford	Saclay
Type of Source	Duoplasmatron	Duoplasmatron	Duoplasmatron	Duoplasmatron	Duoplasmatron
Hydrogen Pressure (Torr)	0.6 - 0.8	0.25	0.2	0.38	0.2
Arc Current (Amperes)	50 - 80	60	5 - 10	45	10 - 40
Maximum Magnetic Field (kG)	2	1.1	2.5	2	3
Source Aperture (mm)	1.8	1.5	0.6	0.8	0.7
Plasma Expansion Cup					
Exit Diam. x Length(mm x mm)	100 x 100	28 x 45	14 x 6	20 x 15	10 x 20
Wall Bias		Auto-bias Extractor serves as a cup*		None	-55V
Cathode Type		Oxide on Ni	Oxide on Ni	Oxide on Ni Gauze	Oxide on Ni Gauze
Duty Factor of Arc	5×10^{-5}	4×10^{-4} (max)	6×10^{-2}	5×10^{-4}	
Lifetime of Source (hours)	>8000	>700	3000	Not known	>6000
Common Cause of Failure			Cathode	Not yet failed in service	Cathode
Extraction					
Directly into Column Field	Into electrostatic	Direct	Direct	Directly into column thru thin extraction electrode	Pierce Extraction before focussing lens.
Into Focussing Lens Section	focussing lens sec.				
Extraction Voltage (kV)	18	350	15 - 27	up to 50	-30
Other Distinctive Source Features	Voltage pulse on intermediate electrode controls shape and amplitude of beam pulse. Pulsed gas shutter at source exit reduces gas throughput by factor of 80.	*Original plasma cup removed. Extractor connected to source anode by 1kΩ resistor.	Pierce anode between cup and extractor run at -200V.		

TABLE II

ACCELERATING COLUMN

Laboratory	Argonne	Brookhaven	CERN Old Linac*	CERN New Linac	Chalk River	Fermilab
Insulator-Electrode Section						
Length of Insulator Stack (cm)	81	114	89.4	121.4	63.6	51.4
Pressurized or Open Exterior	Pressurized	Open	Open	Open	Pressurized	Pressurized
Number of Accelerating Gaps	6	6	2	2	8	8
Overall Gap Length (cm)	18.4	18.7*	12	14	27.0	30, 22.9*
Electrode Apertures (cm)	4.4	2.22 - 3.71	4.8	5	2.6	2.8, 4.2, 3.2**
Electrode Material	Titanium	Titanium	Titanium	Titanium	Ti6Al4V	Titanium
Number of Insulator Rings	6	18	14	19	18	8
ID of Insulator Rings (cm)	45.7	63	50	50	45.8	45.7
Insulator Material	85% Alumina	94% Alumina	Porcelain	Porcelain	96% Alumina	85% Alumina
Mechanical Bonding Material	Epoxy	Epoxy	Araldite	Araldite	Polyvinyl Acetate	Polyvinyl Acetate
Vacuum Sealing Material	Indium Metal Braze*	Indium	Indium	Indium	Polyvinyl Acetate	Polyvinyl Acetate
Voltage Vs Axial Distance, z	$V \sim z$	$V \sim z$			$V \sim z^{4/3}$ to 200kV 31kV/cm for V>200kV	$V \sim z^{4/3}$
Overall Length of Column (cm)	190	120	94.9	126.9	158	213
Voltage-Dividing Resistor	Water	Carbon	Carbon	Carbon	Carbon Film	Water
	*Polarized Proton Column Only	*Thickness of electrodes subtracted.				*22.9cm for beam #3 in Table IV. **Sizes for beams #1,2,3 respectively in Table IV.

Laboratory	ITEP	KEK	Los Alamos	Rutherford New Linac	Saclay
Insulator-Electrode Section					
Length of Insulator Stack (cm)	190	306	50	44.4	45
Pressurized or Open Exterior	Open	Open	Pressurized	Pressurized	Pressurized**
Number of Accelerating Gaps	58	2	16	16	14
Overall Gap Length (cm)	45.0	22	36	44.	43
Electrode Apertures (cm)	40	5.0 - 6.0	4.0	14.0	10
Electrode Material	Stainless Steel	Titanium	Titanium	Titanium	Stainless Steel
Number of Insulator Rings	58	2	14	16	15
ID of Insulator Rings (cm)	50	101	35	21.5	34
Insulator Material	Porcelain	Porcelain	94% Al_2O_3	Pyrex	Alumina
Mechanical Bonding Material	BF-4	None*	Polycarbonate	Polyvinyl Acetate	Vinyl Acetate
Vacuum Sealing Material	Pb	Viton O-Ring	Polycarbonate	Polyvinyl Acetate	Vinyl Acetate
Voltage Vs Axial Distance, z	$V \sim z$	$V \sim z$	$V \sim z^{4/3}$	$V \sim z$	$V \sim z$
Overall Length of Column (cm)	225	330	300	200 (164 cm voltage graded)	52.2
Voltage-Dividing Resistor	Water	RuO_2 Resistor 1700MΩ	Carbon Resistors	Carbon Track Resistors	Organic Liquid Resistor

*The accelerating column consists of two big porcelain tubes, which are not stacks of insulator rings and metal plates. Although cast-metal flanges are cemented at both ends of each tube, the column has no bonding in an ordinary sense.

**Complete ion-source dome and column are in a pressurized tank.

TABLE XII

TRANSITION LINE TO LINAC

Laboratory Line Use	Argonne H^+ or H^-	Argonne Polarized H^+	Brookhaven H^-	CERN Old Linac H^+	CERN New Linac H^+	Chalk River H^+
Length (meters)	5.5	13			6.6	7.5
Number of Bends	0	2 1 Doublet	0	0	0	2 x 45°
Number and Type of Focussing Elements	2 Magnetic Triplets	11 Triplets 1 Singlet (all magnetic)	4 Triplets 2 Matching Quads	2 Magnetic Triplets	4 Triplets 6 Quads (all magnetic)	6 Doublets 1 Triplet (all magnetic)
Lens Apertures (cm)	7.5	10.2 & 7.5	7.5	5	7, 10, 4.8 & 2.9	7.5
Number of Trim or Steering Elements	2	0	2 Pairs	1 Pair	2 Pairs	2 Pairs
Beam Chopper?	Yes	Yes	Yes	No	No	No
Type of Buncher Buncher Aperture (cm)	Single Gap 3.2	Single Gap 3.2	2 Double-Gap Bunchers*	Single Gap 1.8	Double-Drift Harmonic Buncher 2	Single Gap 1.5
Distance of Buncher Gap from First Linac Gap (cm)	190	190	94.6 from last buncher to linac	70	96 & 81 respectively	126
			*78cm between bunchers			

Laboratory Line Use	Fermilab H^+	ITEP H^+	KEK H^+	Los Alamos H^+, H^- Polarized H^+, H^-	Rutherford New Linac H^+	Saclay H^+, D^+, He^+
Length (meters)	3.5	2.95	7	12.0	4.67	4
Number of Bends	0	-	0	4	0	0
Number and Type of Focussing Elements	3 Magnetic Triplets	2 Magnetic Doublets	1 Quadruplet 5 Triplets (all magnetic)	2 Quadrupolets } * 2 Triplets 2 Doublets } ** 2 Singlets (all magnetic)	3 Magnetic Triplets	1 Triplet +5 Lenses (for adaptation)
Lens Apertures (cm)	7.5	4.5	9.08, 7.8, 5.0	* 7.5 **5.0	2 x 9.0 1 x 6.0	7.5
Number of Trim or Steering Elements	0	2 Pairs	2 Pairs	3 Pairs + 2 Vertical	Accel. Column is Mechanically Steerable	0
Beam Chopper ?	Yes	Yes	Yes	Yes	No	Yes
Type of Buncher Buncher Aperture (cm)	Single Gap 3.0	Single Gap 3.8	Coaxial, Double Gaps 3.8	Double-Drift Single Frequency† 2.0	Single Cavity 2.5	Single Gap
Distance of Buncher Gap from First Linac Gap (cm)	80	78	80	150 cm from last Buncher to Linac	80	90
				†6 meters between bunchers		

TABLE IVa

PREACCELERATOR BEAM PROPERTIES

Laboratory	Argonne		BNL	CERN		Chalk River	Fermilab		
Beam	H^+	Polarized H^+	H^+	Old Linac H^+	New Linac H^+	CW H^+	H^+ #1	H^+ #2	H^+ #3
Energy (keV)	750	750	750	510	750	750	750	750	750
Operation Ion Current from Column (mA)	150	0.060	280	330	275	design ~100	165	535	590
Proton Percentage	75 - 80	~50	80	80	75	70-80	85	~80	~80
Current into Linac (mA)	80	0.050	100	190	200 *)	65	140	395	445
Emittance* at Linac Entrance (cm-mrad)	0.3π		0.25π	0.3π	0.3π	Measurements underway	0.2π	0.55π	0.4π
Percentage of Beam	90		90	90	**)	report/Conf.	90	90	90
Method of Emittance Measurement	Slit + multi-strip collectors		Slit + multi-strip collectors	No Permanent Facility	Slit+multiple collector	Pepper Pot Beam pulsed onto plate	Slit + Multi-strip collectors	Slit + Multi-strip collectors	Slit + Multi-strip collectors
Current Out of Linac (mA)	40	0.030	70	80-90	≤150 *)	65	90*	235	270
Emittance* at Linac Exit (cm-mrad)	0.5π		0.6π	0.6π	0.6π		0.7π	1.06π	1.07π
Percentage of Beam	~90		90	90	*) **)		90	90	90
Method of Emittance Measurement	Computed from Beam Profiles		Slit + multi-wire collector	Swept beam on slit+multi-collector(SPES)	Swept beam on slit+multiple collector(SPES)		Computed from wire-scanned Profiles	Computed from wire-scanned Profiles	Computed from wire-scanned Profiles
Buncher Improvement Factor	2	2	> 2	1.8	≥2.5 *)		2	2	2
Pulse Length from Source (μsec)	Up to 550	5000	Up to 400	120	≤220	CW	20	8	7
Pulse Length from Linac (μsec)	Up to 550	Up to 550	Up to 300	100	≤200		15	4	4
Repetition Rate (Hz)	Up to 30	Up to 30	10	1	2		15	15	15
Maximum Current Achieved from Column (mA)	250	0.070-H^+	500	≈600	>300 ***)	45	285	675	650**

*Emittance = Area x βγ

*) Estimated or design value
**) Emittance of full "equivalent beam", i.e., 4 E_{rms}, where E_{rms} is the rms emittance.
***) Limit not yet explored

*Maximum operation linac current for this column was 160 mA for single-turn booster injection.
**Limit not yet explored fully.

Table IVb

PREACCELERATOR BEAM PROPERTIES

Laboratory	ITEP	KEK	Los Alamos			Rutherford	Saclay		
Beam	H^+	H^+	Present Operation H^+	Design Operation H^+	Present Operation H^-	New Linac H^+	H^+	D^+	H_e^+
Energy (keV)	700	750	750	750		665	750	375	~820
Operating Ion Current from Column (mA)	800	600	20	35	0.5	170	40	28	15 (He^+)
Proton Percentage	83 - 85	>80	60	75	$H^-/H_1^+ = 8$ $H^-/H_2^+ = 60$ $H^-/H_3^+ = 32$	Not Known	80	80	
Current into Linac (mA)	450 - 510	230	2.1	21	0.3	135	30	20	~10(He^+)
Emittance* at Linac Entrance (cm-mrad)	0.82π	0.3π	0.04π - 0.06π 99% 0.02π 90%*	0.2π	0.2π	Not Yet Measured	0.1π	0.1π	Not Measured
Percentage of Beam	90	90	99				95	95	
Method of Emittance Measurement	Two-Slit	Single Slit and 24-Segment Detector	Single Slit + multi-segment collector	Single Slit + multi-segment collector	Single Slit + multi-segment collector	Two-Slit	Size of Holes and Wire		
Current Out of Linac (mA)	250	120	1.7	17	0.3	80 at 10MeV	17	6	2
Emittance* at Linac Exit (cm-mrad)	1.5π	0.6π	0.15π - 0.20π 99%		0.5π	Not Yet Measured	0.5π	0.5π	Not Measured
Percentage of Beam	90	90	0.08π 90%*		(100 MeV)		90	90	
Method of Emittance Measurement	Two-Slit	9 Slits and Multi-segment Detector	Single Slit + multi-segment collector			3 Multi-wire Monitors	Size of Holes		
Buncher Improvement Factor	1.7	2	3	3	3	2	2	2	2
Pulse Length from Source (μsec)	50	7 - 25	500	500	500	≤500	400	400	400
Pulse Length from Linac (μsec)	30	0.6 - 20	500	500	500	≤500	400	400	400
Repetition Rate (Hz)	2	1 - 20	120	120	120	1	1	1	1
Maximum Current Achieved from Column (mA)	1500	650	60	60	3.0	200	120		

*Emittance = Area x $\beta\gamma$

*0.05π for 12.5 mA in and 0.12π for 10 mA out at 90% contour. All input beams collimated.

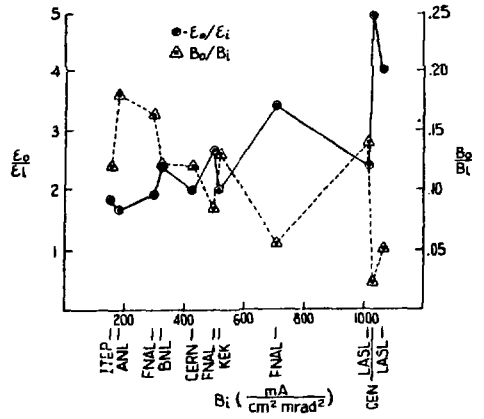

Fig. 2. Ratios of output to input emittance and brightness versus linac imput-beam brightness.

The brightness of the injector beam as a function of current is shown in Fig. 3. One notes the large values for the two Los Alamos and the Saclay beams in the low-current range. Overall there is a reduction in brightness for increasing current, however little if any reduction above ~100 mA. Because both high current and high brightness are desirable in some injectors, the product of injector current times brightness versus current is plotted in the same figure. The increase in this product attests to the modest success of injectors in this regard.

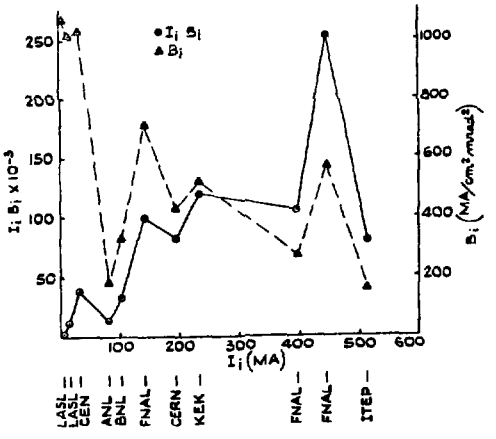

Fig. 3. Injector brightness and current-brightness product as a function of current.

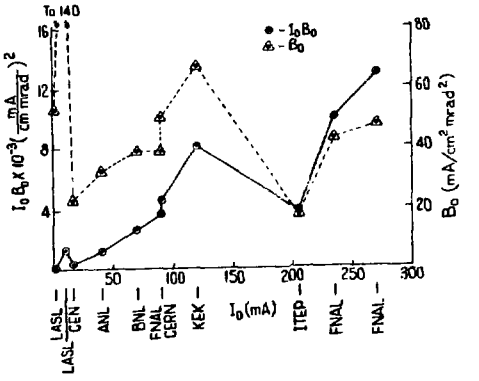

Fig. 4. Linac brightness and current-brightness product as a function of current.

Figure 4 gives a plot of linac-beam brightness versus current up to 270mA. One notes no consistent trend. The product of linac output current and brightness shows again a pronounced general rise with increasing beam current.

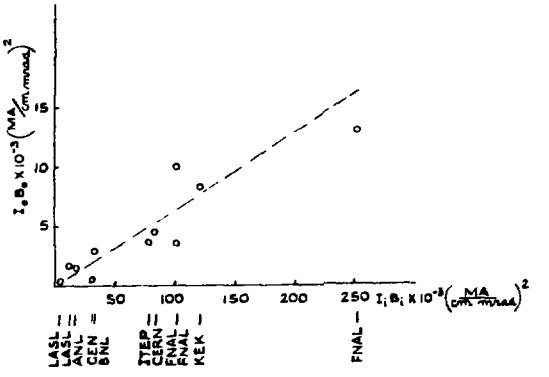

Fig. 5. Linac current-brightness product versus injector current-brightness product.

Finally, in Fig. 5. we show the product of current times brightness for the beam from the linac as a function of the same product for the beam from the injector. There is an apparent proportional relation, as expected from the behavior of the other graphs. The brightest injector beams are in the small-current and small plasma-cup systems at Saclay and Los Alamos. The best performance in terms of current-times-brightness product is clearly in the high-current injectors. The author has played some games with the data. The

TABLE VI

CHARGE-EXCHANGE SOURCES

Lab	Donor	Beam mA (max)	Emitt./π cm mrad
Los Alamos	H_2	0.5(3)	0.2
Novosibirsk	H_2	20	<0.1
	H_2	54	0.2x0.025
	H_2	76, H^-	
	+Na	>100, D^-	
Argonne	H_2	10(19)	~0.1
Livermore	Cs	32 at 1.5keV 18 at 0.7keV D^-	

TABLE VII

H^- DIRECT-EXTRACTION SOURCES

Lab	Type	Aperture mm^2	Beam mA	Emitt./π cm mrad
Novosibirsk	Penning	0.5x10	100(Cs)	~0.1
	Magnetron	0.5x10	100(Cs)	0.08
		1x10	300(Cs)	
		0.5x5	92(Cs)	
		1x30	880(Cs)	
		3x10	1000(Cs)	
Lenigrad	HDDP	4.9	6	.07
Brookhaven	HDDP	4.7	11	0.1
			40(Cs)	0.23
	Magnetron	0.5x10	17	0.14
				~0.19
			45	0.4
		0.5x10	100(Cs)	
		135 (6 slits)	900(Cs)	

reader may wish to play his own to emphasize other aspects of the systems.

Of the complete sets of operational-beam data compiled here the set from KEK is from the newest commissioned injector. The data in beam #2 and #3 in Table IVa for Fermilab are from the latest sequential alterations in that injector over the past several months.

Table I shows that all ion sources in operation are duoplasmatrons with small anode apertures to minimize gas consumption. Rather large plasma-expansion cups serve as an aid in matching the beam to moderately high-gradient columns(Table II). As the cup size increases for the higher current injectors, there is generally a larger emittance. Of interest in this connection is the relatively intense ion-source development over the past several years for thermonuclear application.[2] Much higher ion currents extending to many tens of amperes have been provided. Multi-aperture sources for this purpose appear capable of high-quality beams. In this conference John Osher is reporting a normalized emittance of 0.2π mrad cm for a 500-mA beam from a modified MATS III source.[3] In a single-aperture (1.1cm diameter) source of the same style he obtains an emittance of 0.02π mrad cm for a 100-mA beam. These sources do require relatively large pump capacity, however.

Table IV also shows a polarized-proton beam of 60 μA in operation at Argonne. The atomic-beam-type source has been in operation for three years during which modifications have improved its stability, reliability, and output current.[4] A Lamb-shift source will produce a polarized H^- beam of 0.5 μA peak current when it goes into operation at Los Alamos early in 1977.[5] KEK has a Lamb-shift source which has produced a polarized H^- beam of 0.35 μA with 60% polarization.[6] With developing interest in CW linacs, high-duty-factor injector design is now more critical. The recent development work at Chalk River[7] emphasizes this. It is time to remember the operation many years ago at Oak Ridge with a 1/2-ampere beam at 600kV. Other dc-beam projects now under way include the neutron-source work at LASL with one-ampere T^+ beam at 300kV, at Wisconsin with a 20-mA D^+ beam at 250kV; and at Livermore with a 1/2-ampere D^+ beam at 400kV.

Negative-Ion-Source Development

Negative-ion source currents have increased recently beyond the milliampere to the ampere level.[8,9] There are predominately two types of sources in use and under development. One is charge-exchange sources in which a positive-ion beam is first extracted and then converted in an electron-donor gas cell or jet and direct extraction sources in which negative ions come from reactions within the plasma volume or at metal surfaces. The direct extraction sources of whatever type have their negative-ion yield increased greatly, up to a factor of five, by the introduction of cesium vapor into the sources. There are two recent survey papers on the field of negative-ion production. One paper by Prelec and Sluyters emphasizes direct extraction sources.[10] The later paper by Sluyters covers both charge-exchange and direct-extraction sources.[11]

The performance of some charge-exchange sources (with currents up to 100mA) is presented in Table VI.[11] The beams from two of these sources, Argonne and LASL, are being accelerated in linacs. Argonne is now changing to routine H^- injection into the ZGS at 50MeV.[12] A sodium-vapor jet will be tested in an effort to improve conversion efficiency of the H^+ beams.[13] Testing has started on a compact Penning source, similar to the Novosibirsk design, for future applications at LASL.[14]

The improved yield from a duoplasmatron with a rod on axis to create a hollow discharge as developed by Golubev et.al.,[15] has been developed further at Brookhaven. A detailed and systematic optimization of many source parameters has yielded peak currents of 11mA in the hydrogen mode and 60mA in the hydrogen-cesium mode.[16] Recent measurement of the H^- energy spectrum from this source indicates the primary origin of the ions to be the surface of the rod tip![17] Fig. 6. shows the geometry of the source.

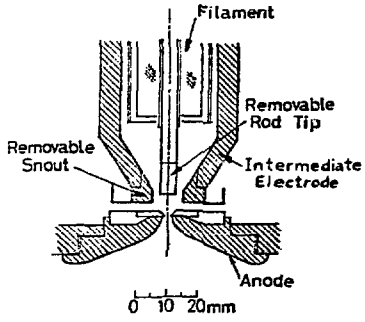

Fig. 6. Hollow-discharge duoplasmatron H^- source.

A great improvement in source development occurred in Dimov's laboratory with the small magnetron source, which was reported in 1972.[18] See Fig. 7 for a schematic source representation. Sources of this kind with an anode emission slit of 0.5mm or longer have achieved H^- current densities at the slit of 0.75A/cm^2. With addition of cesium, the current density reaches 3.7A/cm^2.[19] The bulk of the H^- ions are emitted from the cathode surface, usually molybdenum, under bombardment by fast particles from the plasma discharge. Cesium deposit on the cathode lowers the work function and increases the H^- yield.[19,20] A very narrow cathode-anode gap, down to 0.5mm, prevents destruction of the H^- ions as they are accelerated through the plasma to the anode. A depression in the anode near the emission slit permits fast H^- ions to charge-exchange on neutral atoms into slow H^- ions to charge-exchange on neutral atoms into slow H^- ions there when the gas pressure is sufficiently high. This reduces the H^- ion energy spread. The compact source geometry of the magnetron has been applied to the Penning source in Novosibirsk with similar beam performance. The transverse magnetic field in both the magnetron and Penning sources has the advantage of reducing the extracted electron current.

Brookhaven has reproduced the magnetron and demonstrated similar high-current beams at somewhat lower current densities.[21] Construction of six parallel slits, total area 1.35 cm^2, in the anode permitted

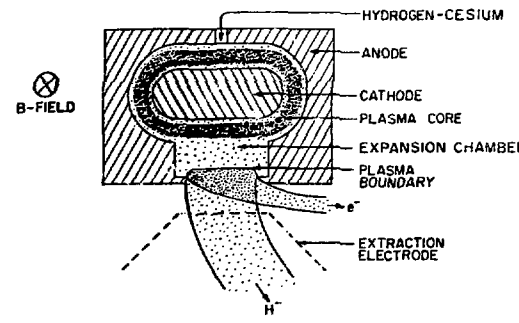

Fig. 7. Magnetron H^- source.

extraction of a 900-mA H^- beam.[9] The primary emphasis at Brookhaven is on production of high-current neutral beams for injection into Tokamaks.

The emittance of these surface-plasma sources (see Table VII), makes them suitable as linac injectors. Consequently Fermilab contracted with Brookhaven for construction of a magnetron. A source, delivered early this year, easily produced in excess of 100mA of negative-ion beam. Since then Fermilab has modified and rebuilt the source to serve better the requirements of shorter pulse length, higher repetition rate and low gas consumption.[22] The result is a source of simple-assembly design, which conditions quickly and operates at 15Hz with a pulse length of 90 μsec and beam currents to 150mA. The volume of the source including connecting channel to a piezoelectric pulsed-gas value is 1.4 cm^3 so that gas consumption is a modest 0.03 Torr liters/sec. Fig. 8. shows a section through the source and Fig. 9. shows a beam pulse.

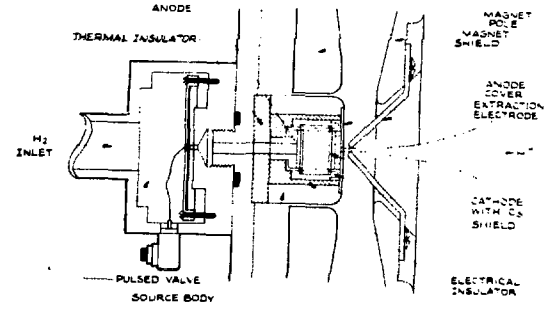

Fig. 8. FNAL MAGNETRON NEGATIVE ION SOURCE

A disadvantage of the small high-current direct-extraction sources is the small size of the beam and its large space-charge forces. Proper handling of this beam following extraction is essential and is being studied. One successful approach in Novosibirsk has been to ex-

tract directly into a 90°-bending and focusing magnet.

Fig. 9. Negative-ion beam pulse from magnetron 20mA x 20 μsec per division.

Conclusions

Most injectors to linacs today use duoplasmatron ion sources with plasma expansion cups. In a comparison among laboratories, the operating beams these injectors deliver to linacs have emittances which, with individual exceptions, increase slowly with increasing beam current so that the product of current and brightness is approximately proportional to beam current.

With the increasing interest in cw linacs, neutron sources and fusion device injectors, there is a continuing and renewed interest in high-current dc sources and accelerating columns that can accomodate the beams.

There is increased usage of a variety of beams in proton linacs now, including H^+, H^-, D^+, He^+, and polarized H^+, and H^- beams. The very significant increase in yield from negative-ion sources in the last few years augurs well for their increased use in the future.

Acknowledgements

The author appreciates the cooperation of contributors from all laboratories who supplied the data presented in Tables I through IV as well as other information which space prevents including.

References

1. Th. Sluyters, Proc. of the 1972 Proton Linear Accel. Conf., Los Alamos, P.283.
2. O.B. Morgan, Proc. of the 2nd Symp. on Ion Sources and Formation of Ion Beams, Berkeley, California (1972), P.VI-1.
3. J.E. Osher and J.C. Davis, proc. of this conf.
4. Everett Parker, Proc. of the Symp. on *High Energy Physics with Polarized* Beams and Targets. (To be published).
5. Edwin P. Chamberlin, Ralph R. Stevens, Jr. and Joseph L. McKibben, proc. of this conf.
6. S. Fukumoto, private communication.
7. J. Ungrin, J.D. Hepburn, M.R. Shubaly, B.G. Chidley and J.H. Ormrod, proc. of this conf.
8. Yu. I. Belchenko, G.I. Dimov and V.G. Dudnikov, Nuclear Fusion 14, 113 (1974)
9. K. Prelec and Th. Sluyters, 6th Symp. on Engineering Problems in Fusion Research, San Diego, P. 430 (1975).
10. K. Prelec and Th. Sluyters, RSI 44, 1451 (1973).
11. Th. Sluyters, Proc. 2nd Symp. on Ion Sources and Formation of Ion Beams. Berkeley, paper VIII-2 (1974).
12. Everett Parker, private communication.
13. H.R. Hiddleston, J.A. Fasolo, D.C. Minette, R.E. Chrien, and J.A. Frederick, proc. of this Conf.
14. Paul W. Allison, private communication.
15. V.P. Golubev, C.A. Nalivaiko, and S.G. Tsepakim, Proc. of 1972 Proton Linear Accel. Conf., Los Alamos, P. 365.
16. M. Kobayaski, K. Prelec and Th. Sluyters, to be published in RSI, Nov. 1976.
17. Th. Sluyters, private communication.
18. Yu. I. Bel'chenko, G.I. Dimov and V.G. Dudnikov, Novosibirsk Report 66-72 (1972).
19. G.I. Dimov, Proc. 2nd Symp. on Ion Sources and Formation of Ion Beams, Berkeley, paper VIII-1 (1974).
20. J.R. Hiskes, Lawrence Livermore Laboratory, Rept. UCID-16765 (1975).
21. K. Prelec and Th. Sluyters, Proc. 2nd Symp. on Ion Sources and Formation of Ion Beams, Berkeley, Paper VIII-6 (1974).
22. C. Schmidt and C. Curtis, proc. of this conf.